IEEE Access
Multidisciplinary ⋮ Rapid Review ⋮ Open Access Journal

Received December 4, 2020, accepted December 16, 2020, date of publication December 21, 2020,
date of current version December 31, 2020.

Digital Object Identifier 10.1109/ACCESS.2020.3045993

Analyzing Polarization Transmission Characteristics in Foggy Environments Based on the Indices of Polarimetric Purity

PENGFEI WANG, DEKUI LI, XINYANG WANG, KAI GUO, YONGXUAN SUN, JUN GAO, AND ZHONGYI GUO
School of Computer and Information, Hefei University of Technology, Hefei 230009, China

Corresponding authors: Kai Guo (kai.guo@hfut.edu.cn) and Zhongyi Guo (guozhongyi@hfut.edu.cn)

This work was supported in part by the National Natural Science Foundation of China under Grant 61775050 and Grant 11804073, in part by the Fundamental Research Funds for the Central Universities under Grant PA2019GDZC0098 and Grant JD2020JGPY0009, and in part by the Anhui Key Laboratory of Polarization Imaging Detection Technology under Grant 2018-KFJJ-02.

ABSTRACT In this paper, we investigated depolarization performance of polarized light in fog scattering system using the indices of polarimetric purity (IPPs) based on the Monte Carlo (MC) algorithm. We compared and analyzed the performances of degree of polarization (DoP) and IPPs in mono-disperse and poly-disperse scattering systems. The depolarization performance of mono-disperse scattering system is dependent on incident infrared wavelength. For the poly-disperse scattering system, the depolarization performance is significantly dependent on the particle-size distributions and the proportion of small particles. These results demonstrate that the IPPs can describe the depolarization performances of disperse systems effectively. It is of great practical significance because it can transmit information in high fidelity better than the DoP.

INDEX TERMS Indices of polarization purity, Monte Carlo algorithm, degree of polarization.

I. INTRODUCTION

Fog is a common phenomenon in our life. In foggy environments, light will be significantly scattered and absorbed by water droplets, and the light intensity information will be attenuated seriously, affecting the transmission efficiency of information [1]. When light transmits in turbid medium, photons will be strongly scattered, decreasing light intensity and making it impossible to obtain useful information through intensity. In contrast, polarization can describe the information since the polarization state of photons could preserve better after scattering. Besides amplitude, phase, spatial distribution [2], [3], polarization is another basic characteristic of electromagnetic wave, which can be utilized to transport information. When light interacts with objects, the polarization state of light will change accordingly, carrying the information of objects. Therefore, it can be used to characterize the target object [4]. In addition, the polarization of light has better transmission characteristics when passing a scattering system. Thus, it is beneficial to explore the polarization transmission characteristics of light in the foggy system, achieving high-fidelity transmission. In recent years, polarization state of light has been widely concerned for its great potential applications in communication [5], [6], navigation [7], [8], detection [9], and imaging [10], [11].

Compared with the traditional imaging method, polarization imaging is more effective in highly scattering system, improving the imaging quality significantly. Schechner *et al.* proposed a physical model and algorithm using polarized light defogging, which achieved good results and has been successfully applied to underwater polarization restoration [12]–[16]. Later, this method has been modified and improved by some other researchers in different scenarios [17]–[21]. Hu *et al.* improved this model and polarization information processing algorithm to effectively solve the following problems: (1) The restoration of objects with high degree of polarization (DoP) (low depolarization) in the scene cannot be realized [17], [19]; (2) Restoration fails in high-concentration scattering environment [18]; (3) The restoration effect is poor in a non-uniform light field environment [20]. Based on the dependence of light scattering on wavelength and the optical correlation theory, Shao *et al.*

The associate editor coordinating the review of this manuscript and approving it for publication was Xinxing Zhou.

proposed a polarization imaging method through highly turbidity water [21]. Xu *et al.* investigated the transmission characteristics of polarization information in different disperse systems in details, such as mono-disperse and poly-disperse scattering systems [22]–[25]. Wang *et al.* studied the polarization characteristics in the cloud disperse system [26], [27] and Zhang *et al.* explored the imaging quality of biological tissues [28], [29].

However, the structure of the atmospheric environment is very complicated, and various particles affect the measurement of polarization parameters. Therefore, researchers are trying to investigate polarization parameters to describe specific microstructures. Among them, Mueller matrix (MM) [22]–[28] has attracted more and more attentions as a characterization method since it can comprehensively reflect the polarization characteristics of media. In the past several years, MM has been preliminarily used in optical communication [22]–[24], polarization imaging [25], [26], and detection of cancer tissues [28]. It has been demonstrated that MM of a medium can be further decomposed into parameters and matrices with physical significance, helping us understand the properties of the MM [30]–[38]. Among them, a set of parameters calculated by the covariance matrix of the Muller matrix is called the indices of polarization purity (IPPs) [31]–[33], which is a comprehensive parameter describing the degree of depolarization of the scattering medium [35]–[37], such as biological tissues [38]. Overall, it has been demonstrated that the IPPs can well describe the depolarization characteristics of the scattering system in different scenarios.

In this work, we have numerically studied the depolarization performances of mono- and poly-disperse scattering systems in the infrared band by using the IPPs, and compared the results with traditional method based on the DoP. In mono-disperse system, the dependence of depolarization performance on the incident wavelengths is studied. In poly-disperse scattering system, we investigate the dependence of depolarization property on the particle size distribution, including the mean values and standard deviations of the scattering particle size.

II. THEORY

A. SIMULATION METHOD

We performed all numerical simulations by using polarized Monte Carlo (MC) algorithm, which has been implemented in calculation of propagation of polarized light in scattering media [39]. A flow-chart including both the main steps of both standard and polarized MC programs is shown in Fig. 1. The steps 1, 2, 3, 4, and 5 are carried out only in the polarized MC program and the other steps should be included in both cases. In step 1, a reference plane is defined to describe the polarization state of light. In step 2, the polarization state of launched photons is defined by Stokes vector. In step 3, the scattering angle θ and azimuthal angle ψ are chosen based on the phase function of the considered scatters and a rejection method. In steps 4 and 5, the reference plane, Stokes

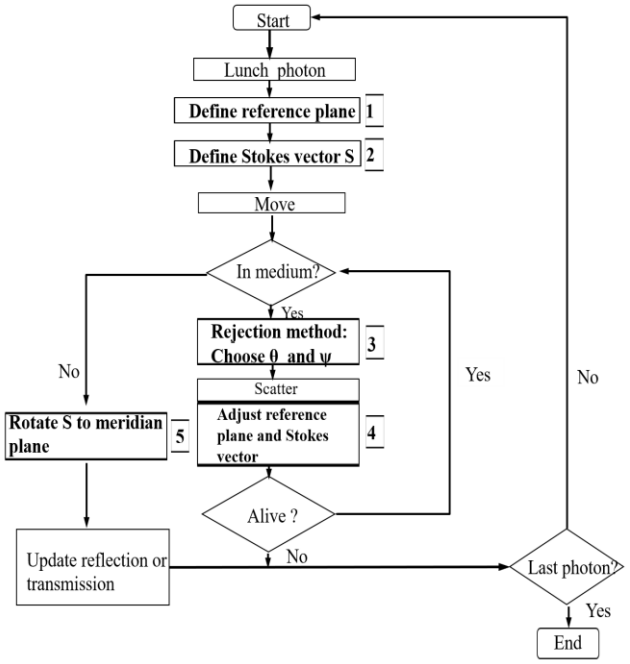

FIGURE 1. Flow chart of polarized MC program.

vector and meridian plane should be updated for each scattering event owing to the randomness of scattering. Further details about the polarized MC method used in the paper can be found in [39].

Stokes vector (S=[I, Q, U, V]^T) is used to describe the polarization of incident light. The DoP notation is usually used in this field and can be expressed as

$$DoP = \frac{\sqrt{Q^2 + U^2 + V^2}}{I} \tag{1}$$

The degrees of linear polarization (DoLP) and degrees of circular polarization (DoCP) can be expressed by the following formulas

$$\begin{cases} DoLP = \dfrac{\sqrt{Q^2 + U^2}}{I} \\ DoCP = \dfrac{|V|}{I} \end{cases} \tag{2}$$

B. INDICES of POLARIMETRIC PURITY

The MM can completely describe the optical properties of a scattering medium. Therefore, it is important to decompose the MM. According to the concept of parallel decomposition of Stokes vectors, we can consider the emitting light as a convex linear combination of several incoherent totally polarized states. The Mueller-Jones matrix can be used to describe a pure non-depolarizing deterministic system, in which the completely polarized incident light will result in emitting light with complete polarization. Due to the one-to-one relation between MM and Hermitian matrix **H**, any parallel decomposition expressed in terms of **H** can be directly translated into the corresponding expression in terms of MM, and vice versa. **H** can be expressed as the following convex

linear combination by four coherency matrices that represent respective pure systems [34], [35]

$$\mathbf{H} = \sum_{i=0}^{3} \frac{\lambda_i}{tr\mathbf{H}} \mathbf{H}_i \tag{3}$$

$$\mathbf{H}_i = (tr\mathbf{H})(u_i \otimes u_i^*) \tag{4}$$

where $\lambda_0 \geq \lambda_1 \geq \lambda_2 \geq \lambda_3 \geq 0$ and μ_I $(i = 0,1,2,3)$ are mutually orthogonal feature vectors, and then the IPPs can be defined by the following equation

$$\begin{cases} P_1 = \dfrac{\lambda_0 - \lambda_1}{\mathrm{tr}\mathbf{H}} \\ P_2 = \dfrac{\lambda_0 + \lambda_1 - 2\lambda_2}{\mathrm{tr}\mathbf{H}} \\ P_3 = \dfrac{\lambda_0 + \lambda_1 + \lambda_2 - 3\lambda_3}{\mathrm{tr}\mathbf{H}} \end{cases} \tag{5}$$

The combination of P_1, P_2, and P_3 forms a three-dimension space and each point in this space can represent depolarization characteristic of a media. For example, the coordinate (0, 0, 0) and (1, 1, 1) correspond to ideal depolarization and non-depolarizing samples, respectively. For other point, the values of the P_1, P_2, and P_3 could be utilized to study the intrinsic depolarizing mechanism. The following quadratic relation between the depolarization index (P) and the three indices of purity (P_1, P_2 and P_3) can be obtained as:

$$P^2 = \frac{1}{3}\left(2P_1^2 + \frac{2}{3}P_2^2 + \frac{1}{3}P_3^2\right) \tag{6}$$

where the greater the absolute value of $\boldsymbol{P}$ is, the better the polarization protection ability of the display medium is.

III. RESULTS AND DISCUSSION

The scattering and absorption of mist particles will not only weaken the intensity of light, but also change the polarization state of incident light. For depicting the photon scattering, we established a realistic fog environment model to simulate the propagation behavior of photon. The incident polarized light travels along the z-axis, and the incident light is a point source, in which the incident wavelength are 3.8μm-4.6μm and 10μm-12μm. We simulated the transmission of light in the scattering medium by emitting photons with number of 10^7 for both ensuring the simulation accuracy and saving time, as schematically shown in Fig. 2.

Considering that the main component of fog is water, thus the refractive index of mist particles is set as $n = 1.33$. We ignored the dispersion of water since the slightly variation on refractive index of mist particles has no significant influence on the performances of DoP and IPPs. The refractive index of atmosphere is set as $n = 1$ because fog usually forms in the atmospheric surface layer with refractive index approaching $n = 1$. We use a semi-infinitely wide detection plane to receive scattered photons from different paths. The transmission distance is L.

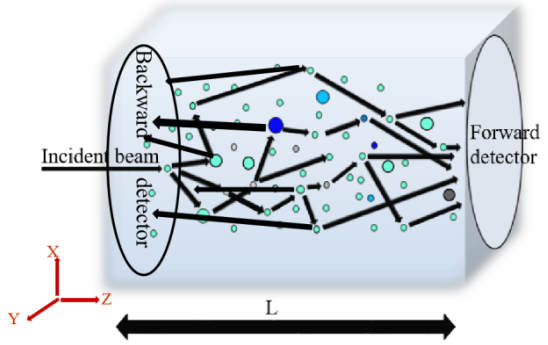

FIGURE 2. The schematic of the MC transport model.

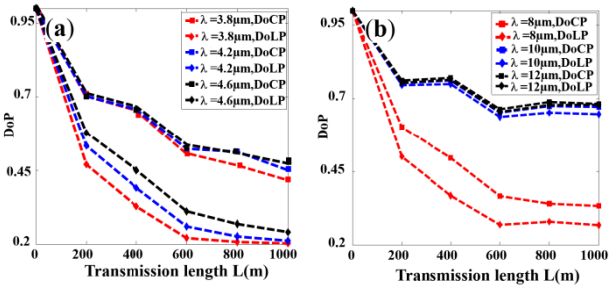

FIGURE 3. The DoP as a function of transmission length L at different incident wavelengths: (a) $\lambda = 3.8\mu$m-4.6μm, (b) $\lambda = 10\mu$m-12μm.

A. MONO-DISPERSE SCATTERING SYSTEM

A mono-disperse scattering system is simulated to explore the depolarization response of the scattering system. The particle radius is $r = 1$ μm and the particle number density is $2.1 \times 10^{-11}/\mu\mathrm{m}^3$. For comparison, the scattering system is illuminated by both circularly polarized light (S=[1,0,0,1]) and linearly polarized light (S=[1,1,0,0]) with wavelengths of 3.8μm-4.6μm and 10μm-12μm. The simulation results are shown in Fig. 3. In the mono-disperse scattering system, as transmission distance increases, both DoCPs and DoLPs decrease in a similar trend. The reductions of DoCPs and DoLPs could be attributed that the photons undergo more collisions in a longer transmission. In addition, the DoCPs and DoLPs increase as the incident wavelength increases. According to the Mie scattering theory, the wavelength increases may result in the decreasing scattering coefficient, so more forward scattered photons could be collected by the detector. Nevertheless, Figs. 3 (a) and 3(b) show that although the DoCPs increases with the increasement of incident wavelength, the change is not significant. Meanwhile, DoCPs and DoLPs show small variations at wavelengths of $\lambda = 10\mu$m and $\lambda = 12\mu$m. Therefore, it is difficult to describe the transmission performance of the scattering system at different wavelengths.

Regarding to this, we use IPPs to study the dependences of the depolarization characteristics of mono-disperse medium on the incident light wavelength and transmission distance. For this purpose, the scattering system is separately

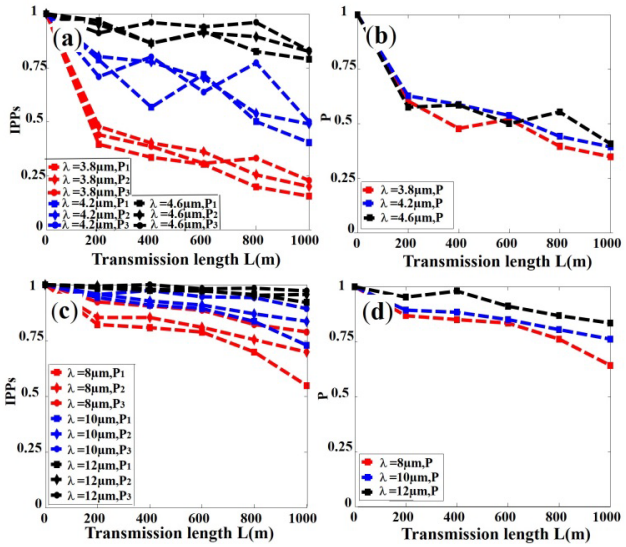

FIGURE 4. The polarization purity index P_1, P_2, P_3 and the polarization purity P change with the transmission length L in the infrared bands of (a), (b) $\lambda = 3.8\mu$m-4.6μm, and (c), (d) $\lambda = 10\mu$m-12μm.

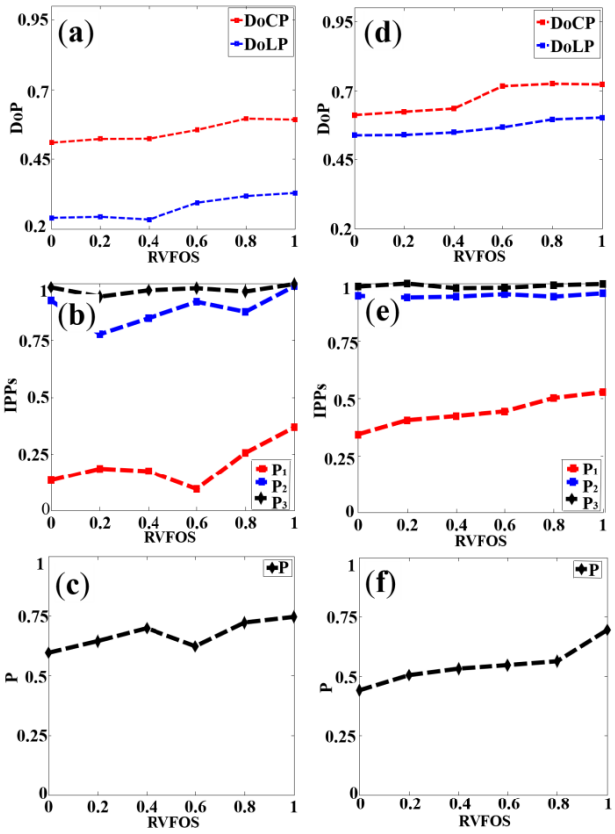

FIGURE 5. The DoP, the polarization purity index P_1, P_2, P_3 and the depolarization index P as the function of the relative volume fraction of small scatter (RVFOS) at different incident wavelength: (a), (b) and (c) $\lambda = 4.2\mu$m; (d), (e) and (f) $\lambda = 10\mu$m.

illuminated by four kinds of light sources, including natural light (S=[1,0,0,0]), horizontally polarized light (S=[1,1,0,0]), 45° linearly polarized light (S=[1,0,1,0]), and circularly polarized light (S=[1,0,0,1]). The simulation results are shown in Fig. 4.

The polarization purity indices P_1, P_2, P_3 and depolarization index P have upward tendency with the increasing incident wavelength. According to the Mie scattering theory, when the incident wavelength increases, the scattering coefficient decreases, and more photons reach the forward detection surface, so the polarization purity of the system increases, and the corresponding system depolarization performance is less. As the transmission distance increases, the photons will collide with more particles, so the number of photons received in the forward direction will decrease. Therefore, the calculated depolarization index $\boldsymbol{P}$ of scattering system will be reduced, and the corresponding depolarization performance will increase. It can be observed that the polarization purity indices P_1, P_2, P_3 and depolarization index $\boldsymbol{P}$ can well describe the depolarization characteristics of the scattering medium. Moreover, a comparison between Fig. 3 and Fig. 4 shows that IPPs can distinguish the depolarization performance of scattering media at different transmission distances and different incident wavelengths better than the DoP. Regarding to this result, we hereafter use IPPs to analyze the depolarization characteristics of poly-disperse scattering media.

B. POLY-DISPERSE SCATTERING SYSTEM

In order to better simulate the real fog environment, we need to construct a scattering medium system composed of a mixture of different particles. We at first mix particles with two different sizes of $r = 1\mu$m and $r = 3\mu$m, and the concentration of the particles is $2.1{*}10^{-11}/\mu\text{m}^3$. The ratio of the number of small particles to the total particle numbers is defined as the mixing ratio. The scattering system is separately illuminated by light source with wavelength of $\lambda = 4.2\mu$m and $\lambda = 10\mu$m. The simulation results are shown in Fig. 5.

In this scattering medium, as shown in Figs. 5 (a) and (d), we can see that DoCP and DoLP increase with increasing mixing ratio, however their changes are smoothly, and cannot describe the depolarization performance of the scattering system under different mixing ratios. In Figs. 5(b) and 5(e), the polarization purity indices P_1, P_2, and P_3 increase as the mixing ratio increases, and they can describe the depolarization performance of the scattering system under different mixing ratios, indicating that the depolarization ability of the scattering medium is gradually reduced with increased mixing ratio. Then we calculated the corresponding depolarization index $\boldsymbol{P}$ and plotted the results in Figs. 5(c) and (f), it can be observed that the value of $\boldsymbol{P}$ also increases as the mixing ratio increases, the larger its value, the smaller the depolarization effect of the scattering system. In other words, the depolarization ability of the scattering medium decreases as the mixing ratio increases. It is because when the

number of small particles in the scattering system gradually increases, the total scattering coefficient decreases and more photons can be received in the forward detection. As a result, the incident polarized light cannot be quickly depolarized into unpolarized light, leading to the decreased depolarization ability of scattering system. The above simulation results show that the depolarization performance of the two-particles mixing system under forward-detection positively depends on the mixing ratio. Figure 5 shows that IPPs can describe the depolarization performance of scattering media under different mixing ratios better than DoP.

In fact, the particle size of a real fog environment follows a certain distribution, which has a certain influence on the depolarization performance of the scattering system. Lognormal distribution is applicable to all random processes and can well reflect the distribution characteristic of the fog particles. Therefore, we investigated a poly-disperse scattering system, where the distribution of particle size can be expressed as the following lognormal distribution [40]

$$N_s = \frac{1}{\sqrt{2\pi}\sigma r} e^{-\frac{[\ln r - \ln R]^2}{2\sigma^2}} \tag{7}$$

where R and σ is the mean value and standard deviation of the distribution inside scattering system, respectively. Equation (7) shows that the sizes and densities of particles depend on the standard deviations σ. We set the mean radius of particles as $R = 1.5\mu$m and the standard deviation as $\sigma = 0.3\mu$m, $\sigma = 0.5\mu$m and $\sigma = 0.7\mu$m. As the standard deviation σ increases, the size distribution of the particles will become wider and the particle spectral density will change accordingly, as shown in Fig. 6.

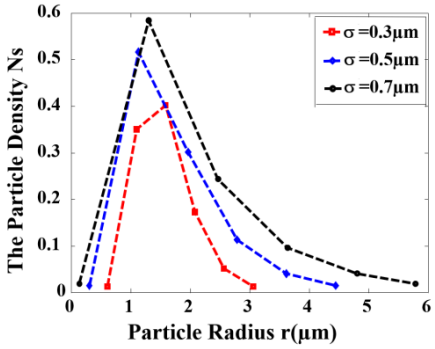

FIGURE 6. The particle spectral distribution N_S with standard deviation of $\sigma = 0.1\mu$m, $\sigma = 0.3\mu$m, $\sigma = 0.5\mu$m and R=1.5μm.

We performed numerical simulations of the poly-disperse scattering system, where the mean value of particles radius is $R = 1.5\mu$m and the standard deviations are $\sigma = 0.3\mu$m, $\sigma = 0.5\mu$m and $\sigma = 0.7\mu$m. The simulation results are plotted in Fig. 7. We can see from Figs. 7 (a) and (d) that DoLPs and DoCPs have minor changes even coincide as the standard deviation σ increases. Therefore, it is difficult to use DoLPs and DoCPs to describe the dependence of depolarization effect of the scattering system on standard deviations. From Figs. 7(b), 7(c), 7(e) and 7(f), we can see that

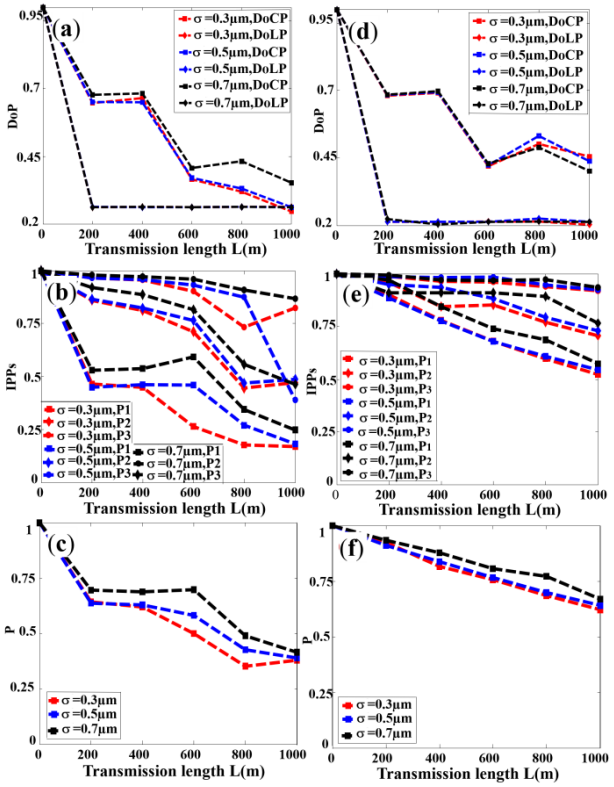

FIGURE 7. The DoP, the polarization purity index P_1, P_2, P_3 and the depolarization index P are functions of transmission length L with different standard deviations: (a), (b) and (c) $\lambda = 4.2\mu$m, (d), (e) and (f) $\lambda = 10\mu$m.

the polarization purity indices P_1, P_2, P_3 and depolarization index $\boldsymbol{P}$ of the scattering system will all become larger when the standard deviation σ increases. This phenomenon shows that in a poly-disperse scattering system, the depolarization performance of scattering systems with same average radius is positively correlated with the standard deviation. When the standard deviation is large, the size of the particles included in the scattering system will increase, as shown in Fig. 6. As a result, the probability of forward scattering increases and more photons could be received by the forward detector. Figure 7 demonstrates that IPPs can describe the dependence of depolarization performance of the scattering system on standard deviation better than DoP.

Overall, the results above show that the depolarization performances of the poly-disperse scattering system significantly depend on the scattering particle radius and the standard deviations of particle size distributions. The most important is that the depolarization performances of the scattering system can be characterized by the IPPs effectively compared to the DoP.

IV. CONCLUSION

In this paper, we numerically investigated the evolution of depolarization performance of polarized light in fog-scattering system by using MC algorithm. We compared

and analyzed the change of DoP and IPPs in different scattering systems, including mono-disperse and poly-disperse scattering systems. For the mono-disperse scattering system, both DoP and IPPs decrease when the transmission distance becomes larger. However, IPPs could distinguish the depolarization responses at different wavelengths better than DoP. In addition, two poly-disperse systems were studied: if there are only two kinds of particles, the depolarization performance depends on the mixing ratio of the particles; if the system has more than two kinds of particles, the depolarization performance will be affected by the standard deviation of the particle size distribution. The above results demonstrate that the IPPs can describe the depolarization performances of disperse systems more effectively. Therefore, the IPPs may be efficient in other polarization technologies, such as the polarization detection, polarization imaging polarization communications and so on.

REFERENCES

[1] D. A. Stewart and O. M. Essenwanger, "A survey of fog and related optical propagation characteristics," *Rev. Geophys.*, vol. 20, no. 3, pp. 481–495, 1982.
[2] X. Liu, L. Liu, F. Wang, and Y. Cai, "Generation of a flexible far-field anomalous hollow beam spot through superposition of two partially coherent sources with different degrees of coherence," *Opt. Commun.*, vol. 428, pp. 69–76, Dec. 2018.
[3] X. Liu, J. Zeng, and Y. Cai, "Review on vortex beams with low spatial coherence," *Adv. Phys., X*, vol. 4, no. 1, Jan. 2019, Art. no. 1626766.
[4] S. L. Jacques, J. R. Roman, and K. Lee, "Imaging superficial tissues with polarized light," *Lasers Surg. Med.*, vol. 26, no. 2, pp. 119–129, 2000.
[5] T. Okoshi, "Polarization-state control schemes for heterodyne or homodyne optical fiber communications," *IEEE Trans. Electron Devices*, vol. 32, no. 12, pp. 2624–2629, Dec. 1985.
[6] M. Martinelli, P. Martelli, and S. M. Pietralunga, "Polarization stabilization in optical communications systems," *J. Lightw. Technol.*, vol. 24, no. 11, pp. 4172–4183, Nov. 2006.
[7] T. Labhart and E. P. Meyer, "Neural mechanisms in insect navigation: Polarization compass and odometer," *Current Opinion Neurobiol.*, vol. 12, no. 6, pp. 707–714, 2002.
[8] M. Sarkar, D. S. S. Bello, C. van Hoof, and A. Theuwissen, "Biologically inspired autonomous agent navigation using an integrated polarization analyzing CMOS image sensor," *Procedia Eng.*, vol. 5, no. 3, pp. 673–676, 2010.
[9] J. Kovac, E. M. Leitch, C. Pryke, J. E. Carlstrom, N. W. Halverson, and W. L. Holzapfel, "Detection of polarization in the cosmic microwave background using DASI," *Nature*, vol. 420, no. 6917, pp. 772–787, 2002.
[10] P. Clemenceau, S. Breugnot, and L. Collot, "Polarization diversity active imaging," *Proc. SPIE*, vol. 3380, pp. 284–291, Sep. 1998.
[11] P. J. Wu and J. T. Walsh, Jr., "Stokes polarimetry imaging of rat tail tissue in a turbid medium: Degree of linear polarization image maps using incident linearly polarized light," *J. Biomed. Opt.*, vol. 11, no. 1, 2006 Art. no. 014031.
[12] Y. Y. Schechner, S. G. Narasimhan, and S. K. Nayar, "Instant dehazing of images using polarization," in *Proc. IEEE Comput. Soc. Conf. Comput. Vis. Pattern Recognit. (CVPR)*, Dec. 2001, p. 1.
[13] Y. Y. Schechner and N. Karpel, "Recovery of underwater visibility and structure by polarization analysis," *IEEE J. Ocean. Eng.*, vol. 30, no. 3, pp. 570–587, Jul. 2005.
[14] E. Namer, S. Shwartz, and Y. Y. Schechner, "Skyless polarimetric calibration and visibility enhancement," *Opt. Exp.*, vol. 17, no. 2, pp. 472–493, 2009.
[15] T. Treibitz and Y. Y. Schechner, "Active polarization descattering," *IEEE Trans. Pattern Anal. Mach. Intell.*, vol. 31, no. 3, pp. 385–399, Mar. 2009.
[16] Y. Y. Schechner, "Inversion by P^4: Polarization-picture post-processing," *Philos. Trans. Roy. Soc. B*, vol. 366, no. 1565, pp. 638–648, 2011.
[17] B. Huang, T. Liu, H. Hu, J. Han, and M. Yu, "Underwater image recovery considering polarization effects of objects," *Opt. Exp.*, vol. 24, no. 9, pp. 9826–9838, 2016.
[18] H. Hu, L. Zhao, X. Li, H. Wang, J. Yang, K. Li, and T. Liu, "Polarimetric image recovery in turbid media employing circularly polarized light," *Opt. Exp.*, vol. 26, no. 19, pp. 25047–25059, 2018.
[19] X. Li, H. Hu, L. Zhao, H. Wang, Y. Yu, L. Wu, and T. Liu, "Polarimetric image recovery method combining histogram stretching for underwater imaging," *Sci. Rep.*, vol. 8, no. 1, Dec. 2018, Art. no. 12430.
[20] H. Hu, L. Zhao, X. Li, H. Wang, and T. Liu, "Underwater image recovery under the nonuniform optical field based on polarimetric imaging," *IEEE Photon. J.*, vol. 10, no. 1, pp. 1–9, Feb. 2018.
[21] F. Liu, P. Han, Y. Wei, G. Zhang, D. Li, and X. Shao, "Polarization imaging, through highly turbid water," in *Proc. Frontiers Opt. Laser Sci.*, Washington, DC, USA, Sep. 2018, p. 139.
[22] Q. Xu, Z. Guo, Q. Tao, W. Jiao, S. Qu, and J. Gao, "Multi-spectral characteristics of polarization retrieve in various atmospheric conditions," *Opt. Commun.*, vol. 339, pp. 167–170, Mar. 2015.
[23] Q. Xu, Z. Guo, Q. Tao, W. Jiao, S. Qu, and J. Gao, "A novel method of retrieving the polarization qubits after being transmitted in turbid media," *J. Opt.*, vol. 17, no. 3, 2015, Art. no. 035606.
[24] Q. Tao, Z. Guo, Q. Xu, W. Jiao, X. Wang, S. Qu, and J. Gao, "Retrieving the polarization information for satellite-to-ground light communication," *J. Opt.*, vol. 17, no. 8, 2015, Art. no. 085701.
[25] Q. Tao, Y. Sun, F. Shen, Q. Xu, J. Gao, and Z. Guo, "Active imaging with the aids of polarization retrieve in turbid media system," *Opt. Commun.*, vol. 359, pp. 405–410, Jan. 2016.
[26] F. Shen, K. Wang, Q. Tao, X. Xu, R. Wu, K. Guo, H. Zhou, Z. Yinc, and Z. Guo, "Polarization imaging performances based on different retrieving Mueller matrixes," *Optik*, vol. 153, pp. 50–57, Jan. 2018.
[27] T. Hu, F. Shen, K. Wang, K. Guo, X. Liu, F. Wang, Z. Peng, Y. Cui, R. Sun, Z. Ding, and J. Gao, "Broad-band transmission characteristics of polarizations in foggy environments," *Atmosphere* vol. 10, no. 6, p. 342, 2019.
[28] F. Shen, B. Zhang, K. Guo, Z. Yin, and Z. Guo, "The depolarization performances of the polarized light in different scattering media systems," *IEEE Photon. J.*, vol. 10, no. 2, Nov. 2017, Art. no. 3900212.
[29] F. Shen, M. Zhang, K. Guo, H. Zhou, Z. Peng, Y. Cui, F. Wang, J. Gao, and Z. Guo, "The depolarization performances of scattering systems based on the indices of polarimetric purity (IPPs)," *Opt. Exp.*, vol. 27, no. 20, pp. 28337–28349, 2019.
[30] J. J. Gil and E. Bernabeu, "Depolarization and polarization indices of an optical system," *Optica Acta Int. J. Opt.*, vol. 33, no. 2, pp. 185–189, 1986.
[31] S. Y. Lu and R. A. Chipman, "Interpretation of Müeller matrices based on polar decomposition," *J. Opt. Soc. Amer. A, Opt. Image Sci.*, vol. 13, no. 5, pp. 1106–1113, 1996.
[32] H. He, N. Zeng, E. Du, Y. Guo, D. Li, R. Liao, and H. Ma, "A possible quantitative mueller matrix transformation technique for anisotropic scattering media/Eine mögliche quantitative Müller-matrix-transformationstechnik für anisotrope streuende medien," *Photon. Lasers Med.*, vol. 2, no. 2, pp. 129–137, Jan. 2013.
[33] R. Ossikovski, A. D. Martino, and S. Guyot, "Forward and reverse product decompositions of depolarizing Müeller matrices," *Opt. Lett.*, vol. 32, no. 6, pp. 689–691, 2007.
[34] F. Moreno and F. González, *Light Scattering From Microstructures*. Laredo, Spain: Springer, 1998.
[35] J. J. G. Perez and R. Ossikovski, *Polarized Light and the Mueller Matrix Approach*. Boca Raton, FL, USA: CRC Press, 2016.
[36] J. J. Gil and I. S. José, "Polarimetric subtraction of Mueller matrices," *J. Opt. Soc. Amer. A, Opt. Image Sci.*, vol. 30, no. 6, pp. 1078–1088, 2013.
[37] J. J. Gil, "Structure of polarimetric purity of a Mueller matrix and sources of depolarization," *Opt. Commun.*, vol. 368, pp. 165–173, Jun. 2016.
[38] A. Van Eeckhout, A. Lizana, E. Garcia-Caurel, J. J. Gil, A. Sansa, C. Rodríguez, I. Estévez, E. González, J. C. Escalera, I. Moreno, and J. Campos, "Polarimetric imaging of biological tissues based on the indices of polarimetric purity," *J. Biophotonics*, vol. 11, no. 4, Apr. 2018, Art. no. e201700189.
[39] J. C. Ramella-Roman, S. A. Prahl, and S. L. Jacques, "Three Monte Carlo programs of polarized light transport into scattering media: Part I," *Opt. Exp.*, vol. 13, no. 12, pp. 4420–4438, 2005.
[40] H. Yorikawa and S. Muramatsu, "Logarithmic normal distribution of particle size from a luminescence line-shape analysis in porous silicon," *Appl. Phys. Lett.*, vol. 71, no. 5, pp. 644–646, Aug. 1997.

PENGFEI WANG received the B.E. degree in electronic information engineering from the Jianghuai College, Anhui University, Hefei, Anhui, China, in 2017. He is currently pursuing the M.S. degree with the Advanced Electromagnetism Function Laboratory (AEMFLab), Hefei University of Technology. His research interest includes infrared polarization information transmission.

DEKUI LI received the B.E. degree in software engineering from Henan Polytechnic University, Jiaozuo, China, in 2019. He is currently pursuing the M.S. degree with the Advanced Electromagnetism Function Laboratory (AEMFLab), Hefei University of Technology. His research interests include polarization imaging and deep learning.

XINYANG WANG received the B.E. degree in information engineering from Fuyang Normal University, Fuyang, China, in 2018. He is currently pursuing the M.S. degree with the Advanced Electromagnetism Function Laboratory (AEMFLab), Hefei University of Technology. His research interest includes polarization information processing.

KAI GUO received the B.S. degree in applied physics and the Ph.D. degree in physics from the Harbin Institute of Technology, Harbin, China, in 2010 and 2015, respectively. From 2015 to 2016, he was a Postdoctoral Research Fellow with Sungkyunkwan University, Suwon, South Korea. From 2016 to 2017, he was a Postdoctoral Research Fellow with The Hong Kong Polytechnic University, Hong Kong, China. He is currently working as an Assistant Professor with the Hefei University of Technology, Hefei, China. His research interests include theoretical surface plasmonics, OAM antenna, OAM communication, light manipulation with metamaterials and metasurfaces, and nonlinear optics.

YONGXUAN SUN received the B.S. degree in communication engineering from Lanzhou Jiaotong University, in 2002, and the Ph.D. degree in signal and information processing from the Hefei University of Technology, Hefei, China, in 2013. He is currently working as an Assistant Professor with the Hefei University of Technology. His research interests include image recognition and processing, polarization information processing, and conventional neural networks.

JUN GAO received the B.S. and M.S. degrees in radio technology and signal and information processing from the Hefei University of Technology, in 1985 and 1990, respectively, and the Ph.D. degree in information and communication engineering from the University of Science and Technology of China, in 1999. He has been a Visiting Scholar with the University of Stuttgart, Germany, and the University of Regina, Canada. He is a Full Professor with the School of Computer and Information, Hefei University of Technology. His research interests include polarization information processing, radar systems, and conventional neural networks.

ZHONGYI GUO received the bachelor's degree from the Department of Physics, Harbin Institute of Technology, in 2003, and the master's and Ph.D. degrees from the Harbin Institute of Technology, in 2005 and 2008, respectively. He was working with the Harbin Institute of Technology. From 2008 to 2009, he worked as an Assistant Professor with the Department of Physics, Harbin Institute of Technology. He held a postdoctoral position with Hanyang University, South Korea, for a period of two years. He held a postdoctoral position with The Hong Kong Polytechnic University, in 2011. He joined with the School of Computer and Information, Hefei University of Technology, as a Full Professor, in the end of 2011. His research interests include advanced optical communication, OAM antenna, polarization information processing, manipulation of optical fields, and nanophotonics.